

Si-induced superconductivity and structural transformations in DyRh₄B₄

A. Köhler¹, G. Behr¹, G. Fuchs^{1#}, K. Nenkov¹, L.C. Gupta^{2*}

¹ IFW Dresden, Leibniz-Institut für Festkörper- und Werkstoffforschung Dresden e.V.,
P.O. Box 270116, D-01171 Dresden, Germany

² Max Planck Institute for the Physics of Complex Systems, D-01187, Dresden, Germany

Abstract

DyRh₄B₄ has been known to crystallize in the primitive tetragonal (*pt*)-structure and to exhibit a ferromagnetic transition at 12 K, the highest magnetic transition temperature in the entire series of the RRh₄B₄ materials [1]. We show here that our silicon-added samples of the nominal composition DyRh₄B₄Si_{0.2} exhibit superconductivity below $T_c \sim 4.5$ K and an antiferromagnetic transition below $T_N \sim 2.7$ K. The 12 K transition observed in the *pt*-DyRh₄B₄ is completely suppressed. Our annealed samples mainly consist of domains of the chemical composition DyRh_{3.9}B_{4.2}Si_{0.08}. These domains contain two crystallographic phases belonging to the body-centred tetragonal (*bct*)-structure and the orthorhombic (*o*)-structure. We have reasons to suggest that superconductivity and antiferromagnetic ordering arise from *bct*-DyRh₄B₄ phase and, therefore, coexist below $T_N \sim 2.7$ K.

Keywords: Superconductors (A); Rare earth alloys and compounds (A); Crystal structure (C); Scanning electron microscopy (SEM) (D); Magnetic measurements (D)

Corresponding author:

G. Fuchs

Leibniz-Institut für Festkörper- und Werkstoffforschung Dresden

P.O. Box 270116, D-01171 Dresden, Germany

Fax: +49-351-4659-490

Tel.: +49-351-4659-538

E-mail: fuchs@ifw-dresden.de

*Visiting scientist

1. Introduction

Kuz'ma et al [2] reported the formation of the borides RM_4B_4 , with R = rare earths, Y and Th and M = Co, in the $CeCo_4B_4$ -type primitive tetragonal (pt) structure, shown in Fig. 1a. These materials exhibit neither a superconducting nor a magnetic transition above 1.5 K. Matthias et al. [3] reported the Rh-based series of ternary materials RRh_4B_4 crystallizing in the pt - $CeCo_4B_4$ -structure. These materials generated great interest not only because the two nonmagnetic members of this series, $LuRh_4B_4$ and YRh_4B_4 , superconduct with high T_c (> 10 K) but also because several members of this series (with R = Nd, Sm, Er, Tm) exhibit simultaneously both superconductivity and long range magnetism. These materials, therefore, have been studied extensively for the interplay of superconductivity and magnetism [1]. Materials with composition RM_4B_4 crystallizing in structures *other than the* pt - $CeCo_4B_4$ -type have also been reported. For example, RRu_4B_4 crystallize in the bct -tetragonal structure, see Fig. 1b; none of them, except $LuRu_4B_4$ ($T_c \sim 1.8$ K), exhibits superconductivity [4]. “Mixed materials” with composition $R(Rh_{1-x}Ru_x)_4B_4$ ($x \sim 0.15$) crystallize, essentially as single phase, in the bct - $LuRu_4B_4$ structure; those with heavy rare earths (R = Lu, Tm, Er, Ho, Dy) superconduct [4].

bct - $ErRh_4B_4$ has been synthesized and studied. It does exhibit superconductivity ($T_c \sim 7.8$ K) as in pt - $ErRh_4B_4$. However, instead of ferromagnetic ordering in pt - $ErRh_4B_4$, bct - $ErRh_4B_4$ undergoes an antiferromagnetic ordering below $T_N = 0.65$ K [5]. bct - $ErRh_4B_4$ has also been produced by carbon-doping ($T_c \sim 7.5$ K and $T_N \sim 0.9$ K) [6]. $LuRh_4B_4$ was reported forming in yet another structure, an orthorhombic structure known in literature as o - $LuRh_4B_4$ [7]. The structure is shown in Fig. 1c. Some materials of the composition RRh_4B_4 (R = heavy rare earths such as Ho, Er, Tm, Yb, Lu) have been synthesized crystallizing in the o - $LuRh_4B_4$ and their magnetic and superconducting properties have been reported [8]. $DyRh_4B_4$ and YRh_4B_4 have been produced in the bct - $LuRu_4B_4$ structure using high pressure synthesis route [9]. A significant result of this work was the observation of superconductivity in bct - $DyRh_4B_4$ at T_c

~ 4.5 K. A ferromagnetic transition at a rather high temperature, $T_M \sim 40$ K, was also observed in *bct*-DyRh₄B₄ [9]. The superconducting and magnetic ordering temperatures reported for ErRh₄B₄ and DyRh₄B₄ are listed in Table 1.

Recently, superconductivity was reported at $T_c \sim 10$ K in multiphase materials of the quaternary system Y-Rh-B-Si [10]. As we mentioned above, *bct*-DyRh₄B₄ and *bct*-ErRh₄B₄ have superconducting and magnetic properties that are remarkably different from those of *pt*-DyRh₄B₄ and *pt*-ErRh₄B₄. Such considerations motivated us to try another chemical route, namely, the effect of introducing Si, to promote the structural transformation *pt* \rightarrow *bct* among the members of the series RRh₄B₄. DyRh₄B₄ was chosen in the present work for such studies.

2. Experimental

Polycrystalline samples of nominal composition DyRh₄B₄Si_x ($x = 0, 0.1$ and 0.2) were synthesized by arc-melting. The as-prepared ingots were wrapped in tantalum foils and annealed at 1100°C for 72 hours in an evacuated silica tube. Final composition and the phases present in the samples were checked and studied by electron probe microanalysis. Powder X-ray diffraction was used to determine the crystal structures of the major phases present in our materials. Magnetic and superconducting properties of the as-cast and the annealed samples were measured using Quantum Design PPMS and SQUID magnetometers.

3. Results and discussion

The AC-susceptibility measurements, shown in Fig. 2, of the sample DyRh₄B₄ (with no added silicon) reveal the well known ferromagnetic transition at ~ 12 K in this material [3]. Inset in Fig. 2 shows the corresponding hysteresis curve in the ferromagnetic state at $T = 2$ K. The temperature dependence of the inverse DC susceptibility of this samples shows Curie-Weiss behavior between 300 K and 50 K with a Curie-Weiss temperature of 18.0 K and an effective

magnetic moment of $\mu_{\text{eff}} = 10.4 \mu_B$ per Dy^{3+} ion which is slightly below the free ion value of $10.63 \mu_B$ per Dy ion. Similar data have been reported already for *pt*- DyRh_4B_4 [3].

In Fig. 2, there are, besides the main peak at 12 K, two other maxima at 23 K and 37 K in the AC-susceptibility curve. We shall comment upon them below when we discuss the results of the microanalysis of the samples.

AC-susceptibility measurements of the as-cast $\text{DyRh}_4\text{B}_4\text{Si}_{0.2}$ sample, Fig. 3a, show a superconducting transition at $T = 4.5$ K with a large diamagnetic response. As can be seen from Fig. 3a, the ferromagnetic transition (at ~ 12.3 K) observed in silicon-free sample has vanished. Further, we see a peak at 37 K in this silicon-added as-cast sample also¹. It is remarkable that this magnetic transition vanishes in the annealed sample, see Fig. 3b. The volume fraction of the superconducting part in this sample was determined as $\sim 50\%$ by means of the slope of the field dependent magnetization curve in the Meißner state.

The sample $\text{DyRh}_4\text{B}_4\text{Si}_{0.1}$ with lower silicon content also superconducts below 4 K. However the superconducting volume fraction in this case is only 7%. A magnetic transition is observed at $T_M = 12$ K in the as-cast sample indicating that a small fraction of *pt*- DyRh_4B_4 phase still continues to exist in the material. This transition disappears in the annealed sample and the magnetic transition observed below $T_N = 2.7$ K survives. Thus, the two annealed samples $\text{DyRh}_4\text{B}_4\text{Si}_{0.1}$ and $\text{DyRh}_4\text{B}_4\text{Si}_{0.2}$ have similar superconducting and magnetic properties, except for the low superconducting volume fraction in the sample $\text{DyRh}_4\text{B}_4\text{Si}_{0.1}$. In the following we shall focus our attention on the material $\text{DyRh}_4\text{B}_4\text{Si}_{0.2}$ only.

Electron probe microanalysis of the as-cast and the annealed samples has been carried out. The insets in Figs. 3a and 3b show the backscattered electron (BSE) images of the superconducting $\text{DyRh}_4\text{B}_4\text{Si}_{0.2}$ samples (as-cast sample in Fig. 3a and the annealed sample in Fig. 3b). The gray regions, which form the most part of the samples, have the composition

¹As pointed out earlier, a similar peak is observed in our as-cast silicon free sample DyRh_4B_4 , Fig. 2.

$\text{DyRh}_{3.9}\text{B}_{4.6}\text{Si}_{0.08}$ in the as-cast and $\text{DyRh}_{3.9}\text{B}_{4.2}\text{Si}_{0.08}$ in the annealed sample. Added silicon is not fully incorporated (the assimilated silicon is lower than the silicon taken to start with). White regions correspond to the compositions $\text{DyRh}_{3.1}\text{B}_{2.5}\text{Si}_{0.05}$ in the as-cast and $\text{DyRh}_{3.0}\text{B}_{2.0}\text{Si}_{0.35}$ in the annealed samples. This secondary phase can be identified as a related phase to the mother compound DyRh_3B_2 with monoclinic ErIr_3B_2 -type structure [11] (also see Table 2.9 in [8]). During the annealing process, amount of this 132-phase is considerably reduced which is obvious by comparing the two BSE images (insets of Figs. 3a and 3b). Simultaneously the magnetic transition at $T_M = 37$ K (Fig. 3a) vanishes. Thus we conclude that this magnetic transition is caused by the secondary phase inclusions. This thesis is supported by our magnetic measurements on samples of nominal composition of $\text{DyRh}_{3.0}\text{B}_{2.0}\text{Si}_{0.2}$. Similar behaviour has been observed in ErIr_4B_4 compound [11]. Likewise, the additional maxima in Fig. 2 are attributed to the presence of some other minority impurity phases.

The magnetic phase diagram of $\text{DyRh}_4\text{B}_4\text{Si}_{0.2}$ in the H - T plane shown in Fig. 4 reveals bulk superconductivity in the measured temperature range between T_c and 2 K below the upper critical field $H_{c2}(T)$. The magnetization in the superconducting state was investigated as function of temperature in the zero-field cooling (*zfc*) and in the field cooling (*fc*) mode applying magnetic fields up to 0.1 T. A peak in the *fc* branch of the *dc* susceptibility appearing at nearly the same temperature T^* for each applied field announce magnetic ordering at this temperature, i.e. $T_N = T^* \approx 2.7$ K (see Fig. 4). The irreversibility field determined from these data was found to increase with decreasing temperature in the paramagnetic state. The range between H_{irr} and H_{c2} in which the magnetization remains reversible occupies a large range of the magnetic phase diagram indicating the weak flux pinning properties of the investigated sample.

According to Fig. 4, superconductivity and antiferromagnetism are found to coexist in $\text{DyRh}_4\text{B}_4\text{Si}_{0.2}$ at temperatures below $T_N \approx 2.7$ K. Note that the slope dH_{c2}/dT of the $H_{c2}(T)$

curve becomes larger below T_N , i.e. the superconducting properties are observed to improve in the antiferromagnetically ordered state. The coexistence of superconductivity and antiferromagnetism was additionally confirmed by magnetization vs. field measurements performed at temperatures below T_N . The magnetization data plotted in Fig. 5 show both superconductivity at magnetic fields below about 0.4 T (including the Meissner effect at very low fields and a hysteretic behaviour due to flux pinning in the field range up to about 0.2 T) and the non-hysteretic antiferromagnetic “background” which becomes visible at fields $H > H_{c2}$. The highly non-linear $M(H)$ dependence above $\mu_0 H \approx 1$ T (see inset in Fig 5) corresponds to the Brillouin function describing the magnetization of the paramagnetic phase at a large ratio $\mu_B H/kT$.

X-ray powder diffraction pattern of the annealed $\text{DyRh}_4\text{B}_4\text{Si}_{0.2}$ sample is shown in Fig. 6a. This pattern consists of the expected pattern of the *bct*- LuRu_4B_4 crystal structure type (blue reference diffraction pattern shown in Fig. 6b) and it also has intense additional diffraction lines, for example, at $2\theta = 36.5^\circ$ and $2\theta = 39^\circ$. We identified these as originating from the orthorhombic polytype of DyRh_4B_4 (red reference pattern of *o*- LuRh_4B_4 in Fig. 6b, the appropriate crystal structure is drawn in Fig. 1c). It is to be pointed out here that the occurrence of the *o*- LuRh_4B_4 type structure in DyRh_4B_4 has not been reported so far in literature. Since we find a mixture of the two polytypes *bct*- DyRh_4B_4 and *o*- DyRh_4B_4 , closely related to each other, we conclude that the assimilation of silicon in DyRh_4B_4 causes the formation of both of these polytypes. This is in contrast to the effect of C added to ErRh_4B_4 wherein only the *bct*-type structure is stabilized [6]. It appears to us that silicon may be entering in *more than one* crystallographic sites in DyRh_4B_4 . In dependence on which crystallographic site silicon is incorporated, the *bct*-phase or the *o*-phase will be favoured. This generates in the sample a mixture of the two phases. It would be of interest to study

further this phenomenon, namely, *an impurity atom stabilizing two crystallographic structures* in the RRh_4B_4 system.

We attribute the superconducting transition at 4.4 K to the bct - $DyRh_4B_4$ for the following reasons: It is known [4] that $Dy(Rh_{0.85}Ru_{0.15})_4B_4$ crystallizes in the bct - $LuRu_4B_4$ structure and superconducts at $T_c \sim 4.0$ K. Further, according to the recent work [9], bct - $DyRh_4B_4$ (high pressure route) exhibits superconductivity at ~ 4.5 K. In both cases, T_c is close to that found in our work. Similar results are available in the case of $ErRh_4B_4$. bct - $ErRh_4B_4$ has been obtained through two routes, high pressure synthesis [5] and incorporation of C [6]. Superconducting and magnetic properties of the resulting bct - $ErRh_4B_4$ are nearly same. These two examples suggest that the observed superconducting and magnetic properties are specific to the phase rather than the route followed to realize that phase and this is what it should be. Thus it is quite reasonable to propose that it is the bct -phase of $DyRh_4B_4$ that is responsible for the observed superconductivity in $DyRh_4B_4Si_{0.2}$. Further support to our proposal comes from our own studies on the annealed material $DyRh_4B_4Si_{0.1}$. X-ray powder diffraction of this sample shows that it contains a *higher* fraction of the orthorhombic phase while the superconducting volume fraction is much lower than that in the $DyRh_4B_4Si_{0.2}$ sample. Magnetic response of $DyRh_4B_4Si_{0.1}$ is also much weaker than that of $DyRh_4B_4Si_{0.2}$. This observation motivates us to suggest that the magnetic transition that we see in $DyRh_4B_4Si_{0.2}$ also arises from the bct - $DyRh_4B_4$, implying thereby coexistence of superconductivity and antiferromagnetism in bct - $DyRh_4B_4$ below $T_N \sim 2.7$ K. In Table 2, our data are compared with reported data for pt and bct $DyRh_4B_4$ [1,4,9]. More work is required to be able to comment upon the superconducting/magnetic properties of o - $DyRh_4B_4$.

4. Conclusions

In conclusion, we report here the results of our studies of incorporation of Si in $DyRh_4B_4$. Our work shows that samples of nominal composition $DyRh_4B_4Si_{0.2}$ have two structural phases,

bct-DyRh₄B₄ and *o*-DyRh₄B₄. We attribute the observed superconductivity at $T_c \sim 4.4$ K and antiferromagnetic transition at $T_N \sim 2.7$ K in DyRh₄B₄Si_{0.2} to the *bct*-DyRh₄B₄ which implies coexistence of superconductivity and magnetic order below 2.7 K in this phase.

As we do not see any magnetic transition in the vicinity of 37 K in our annealed samples which have *bct*-DyRh₄B₄, it appears to us that the reported magnetic transition at 40 K in the *bct*-DyRh₄B₄ [9] is most probably due to the presence of the DyRh₃B₂ which is known to exhibit [11] a magnetic transition at ~ 37 K.

It would be of interest to extend this study to other members of the *RRh*₄B₄-series, namely, to try to incorporate suitable elements in the matrix *RRh*₄B₄ and study the structural transformation(s) and superconducting and magnetic properties of the resulting phases of *RRh*₄B₄.

Acknowledgements

The authors would like to thank S. Müller-Litvanyi, S. Pichl and A. Ostwaldt for technical support and J. Dshemuchadse, T. Leisegang and W. Löser for fruitful discussions. The financial support of the Deutsche Forschungsgemeinschaft within the SFB 463 „Rare-Earth Intermetallics: Structure, Magnetism and Transport“ is grateful acknowledged. LCG thanks MPIPKS for providing support and hospitality during his several visits. He also thanks Humboldt Foundation for the support during some of his visits to MPIPKS.

References

- [1] For an extensive review on the magnetic and superconducting properties on the ternary superconductors, including RRh_4B_4 , see, for example, Ø. Fischer, in *Ferromagnetic Materials*, Eds. K. H. J. Buschow and E. P. Wohlfarth (Elsevier Science Publishers B. V. 1990) Vol. 5, Chapter 6.
- [2] Yu B. Kuz'ma, N. S. Bilonizhko, *Sov. Phys. Crystallogr.* 16, 897 (1972)
- [3] (a) B. T. Matthias, E. Corenzwit, J. M. Vandenberg, H. Barz, *Proc. Natl. Acad. USA*, 74, 1334 (1977); (b) J. M. Vandenberg and B. T. Matthias, *Science* 198, 194 (1977); (c) H. B. MacKay, L. D. Woolf, M. B. Maple, D. C. Johnston, *J. Low Temp. Phys.* 41, 639 (1980)
- [4] D. C. Johnston, *Solid State Commun.* 24, 969 (1977)
- [5] H. Iwasaki, Y. Muto, *Phys. Rev. B* 33, 4680 (1986); H. Iwasaki, M. Isino, Y. Muto, *Physica* 108 B, 759 (1980)
- [6] J. L. Genicon, A. Sulpice, R. Tournier, B. Chevalier, J. Etourneau, *J. Physique-Letters* 44, L725 (1983)
- [7] K. Yvon, D. C. Johnston, *Acta Cryst. B* 38, 247 (1982)
- [8] D. C. Johnston, H. F. Braun, in *Superconductivity in Ternary Compounds II*, Eds. M. B. Maple and Ø Fischer (Springer, New York, 1982), p. 11
- [9] A. J. Zaleski, A. V. Tswyashchenko, E. P. Khlybov, L. N. Fomicheva, I. E. Kostyleva, S. A. Lachenkov, O. G. Zamolodchikov, paper presented at the 24th International Conference on Low Temperature Physics, Proceedings edited by Y. Takeda, S. P. Hirshfeld, S. O. Hill, P. J. Hirshfeld, A. M. Goldman (American Institute of Physics, 2006), CP. 850
- [10] Ashwini K. Jain, G. V. M. Kiruthika, V. Bhattacharya, L. C. Gupta, *Solid State Commun.* 131, 261 (2004)
- [11] H.C. Ku, G. P. Meisner, *J. Less-Common Metals* 78 (1981) 99

Tables

Table 1

Superconducting (T_c) and magnetic transition temperatures (T_N , T_M) of ErRh_4B_4 and DyRh_4B_4

	ErRh_4B_4			DyRh_4B_4		
	<i>pt</i>	<i>bct</i>	<i>o</i>	<i>pt</i>	[*] <i>bct</i>	[♦] <i>bct</i>
T_c / K	8.7	7.8	4.5		4.0	4.5
T_N / K		0.65	0.3		1.5	
T_M / K	0.9			12.0		40

^{*}*bct*- $\text{Dy}(\text{Rh}_{1-0.15}\text{Ru}_{0.15})_4\text{B}_4$ [4], [♦]*bct*- DyRh_4B_4 high pressure synthesis compound [9]; the orthorhombic crystal structure was reported in literature for ErRh_4B_4 but not for DyRh_4B_4 .

Table 2

Superconducting (T_c) and magnetic transition temperatures (T_N , T_M) of DyRh_4B_4

DyRh_4B_4						
	<i>pt</i>	<i>pt</i>	[*] <i>bct</i>	[♦] <i>bct</i>	<i>bct</i>	<i>o</i>
T_c / K			4.0	4.5	4.4	< 2K
T_N / K			1.5		2.7	
T_M / K	12.0	12.3		40		

^{*}*bct*- $\text{Dy}(\text{Rh}_{1-0.15}\text{Ru}_{0.15})_4\text{B}_4$ [4], [♦]*bct*- DyRh_4B_4 high pressure synthesis [9], our work in bold.

Figure Captions

Figure 1

Lattice polytypes of the materials RRh_4B_4

a) $CeCo_4B_4$ -type primitive tetragonal structure (45° rotated)

b) $LuRu_4B_4$ -type body centered tetragonal structure

c) $LuRh_4B_4$ -type orthorhombic structure

All polytypes consist of the same rare earth (orange balls) sub-lattice, but different orientations of the Rh (dark blue balls) and B (light blue balls) polyhedra, which is marked by different colours of the polyhedra; please note: the rare earth element is not inside the polyhedra but above in next layer; the unit cell is marked by a frame.

Figure 2 (colour online)

AC-susceptibility of the $DyRh_4B_4$ as-cast sample,

inset: magnetic hysteresis curve at $T = 2$ K.

Figure 3 (colour online)

AC-susceptibility of the a) as grown and b) annealed $DyRh_4B_4Si_{0.2}$ sample,

inset: backscattered electron (BSE) images.

Figure 4 (colour online)

Temperature dependence of the upper critical field H_{c2} of the annealed $DyRh_4B_4Si_{0.2}$ sample (solid line, blue circles) as determined from the onset of superconductivity of *ac* susceptibility data. Dotted line: antiferromagnetic ordering temperature T_N corresponding to the temperature T^* (red circles) at which a peak appears in the field cooling branch of the *dc* susceptibility; dashed line (open circles): irreversibility field H_{irr} . Coexistence of superconductivity and antiferromagnetism is observed below T_N .

Figure 5 (colour online)

Field dependence of the magnetic moment of the annealed $DyRh_4B_4Si_{0.2}$ sample measured at $T = 2$ K below $T_N = 2.7$ (see Fig. 4). Superconductivity in the magnetically ordered state is indicated by the diamagnetism at low applied fields (Meissner state) and the hysteretic character of the magnetization loop.

Figure 6

a) X-ray powder diffraction pattern (θ - 2θ scan) of the annealed $DyRh_4B_4Si_{0.2}$

b) comparison of the peaks of the measured diffraction pattern (upper panel) with the peaks of the three reference patterns: *bct*- $LuRu_4B_4$ (blue), *o*- $LuRh_4B_4$ (red) and *pt*- YRh_4B_4 (green)

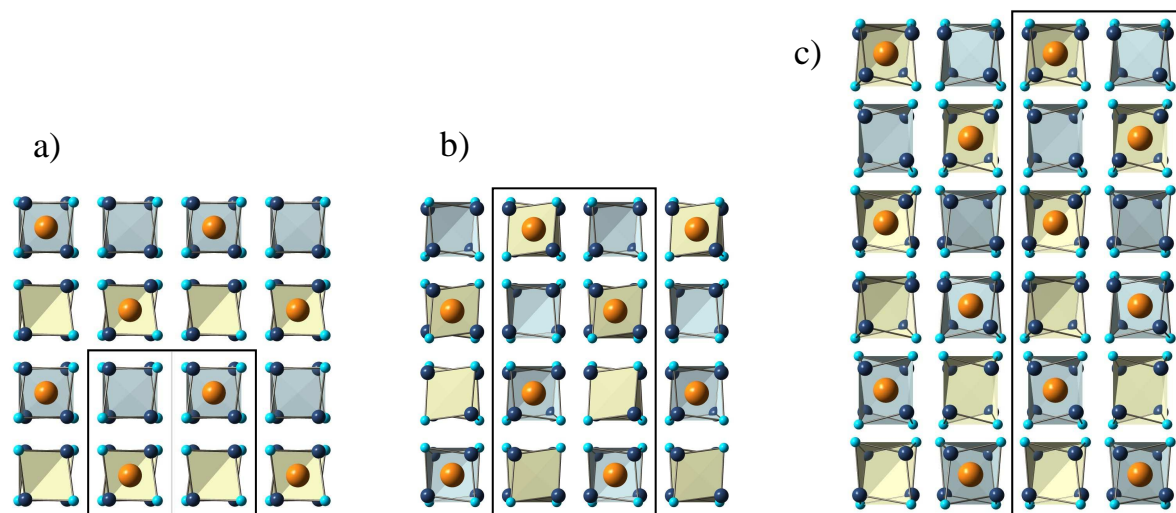


Fig. 1

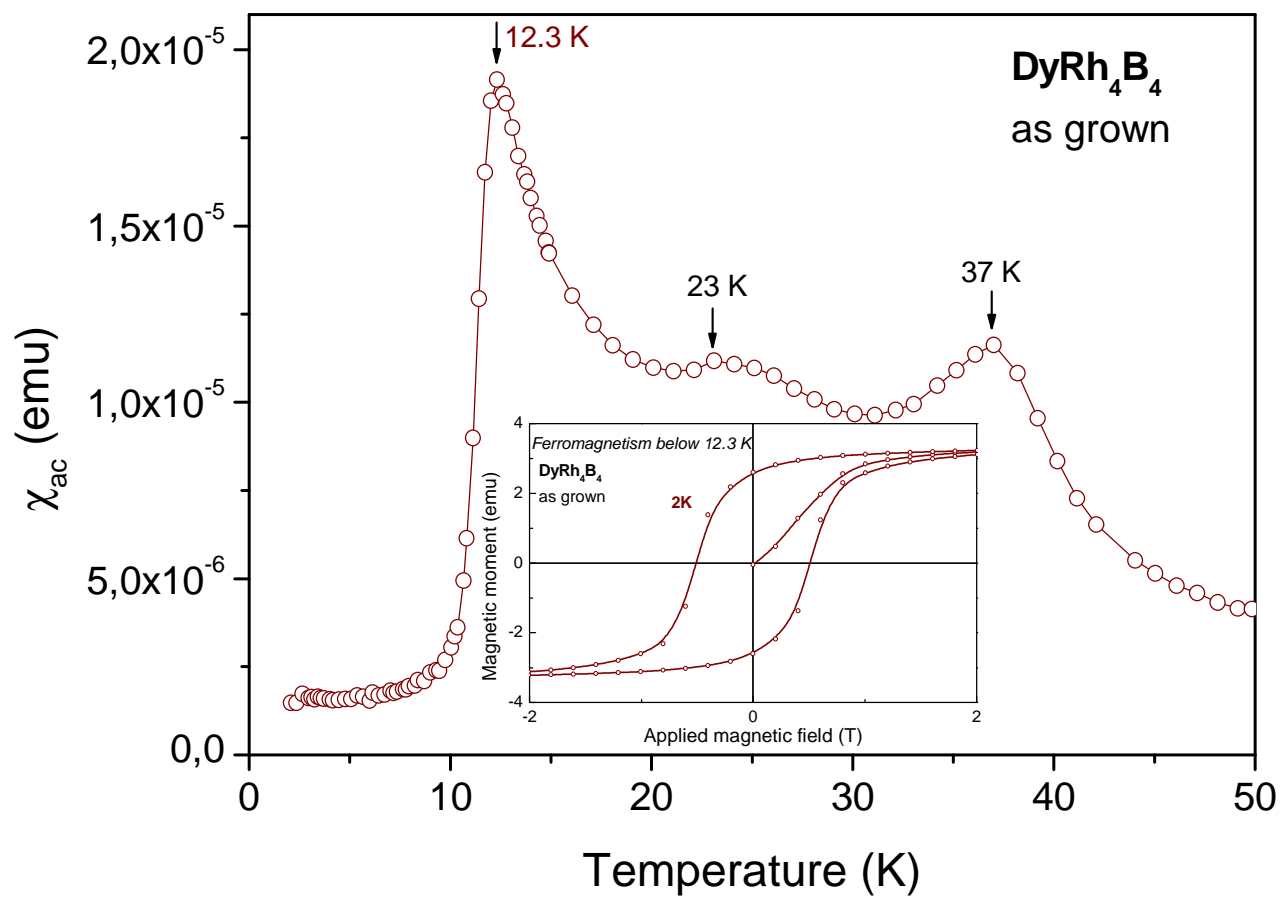


Fig. 2

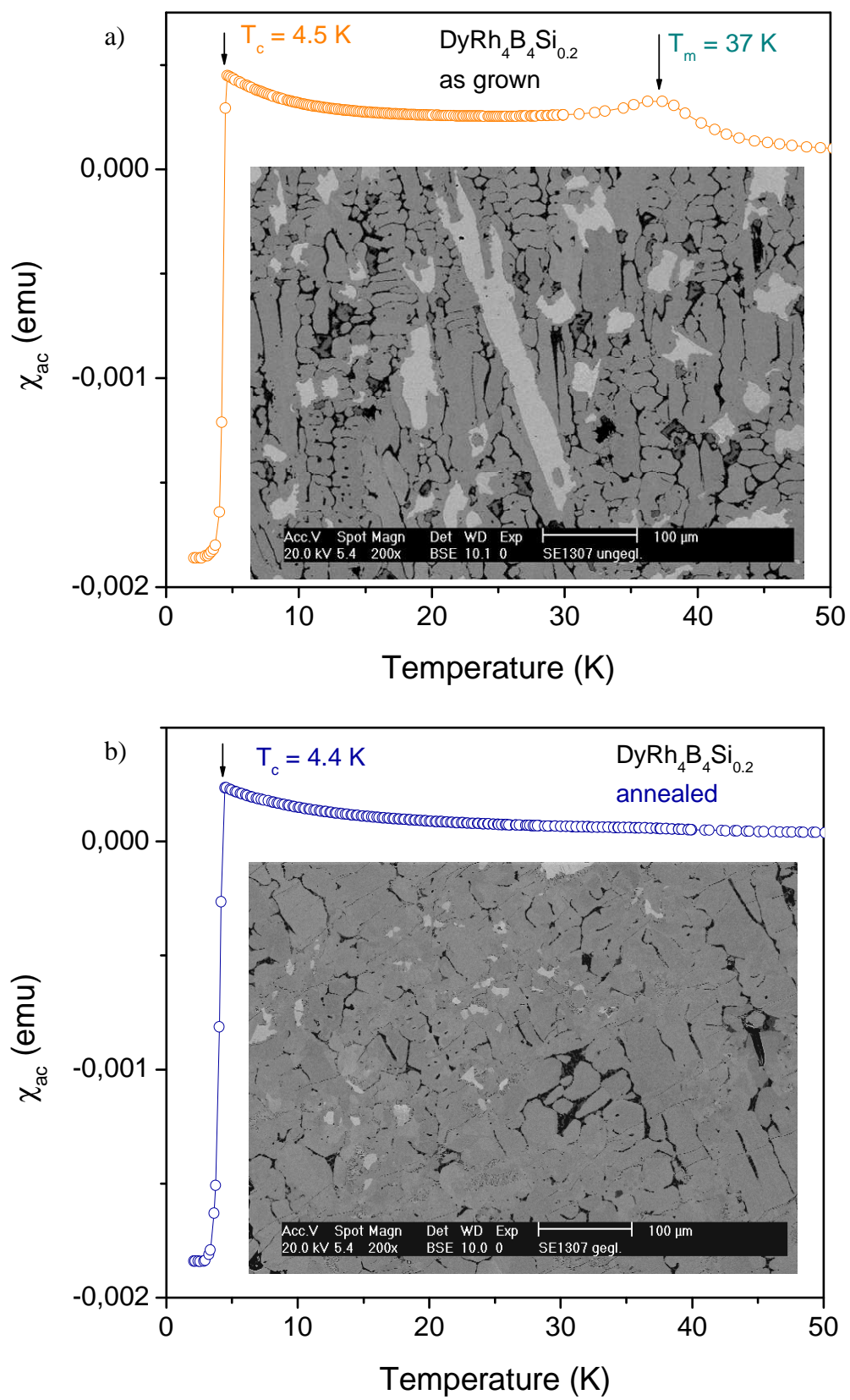


Fig. 3

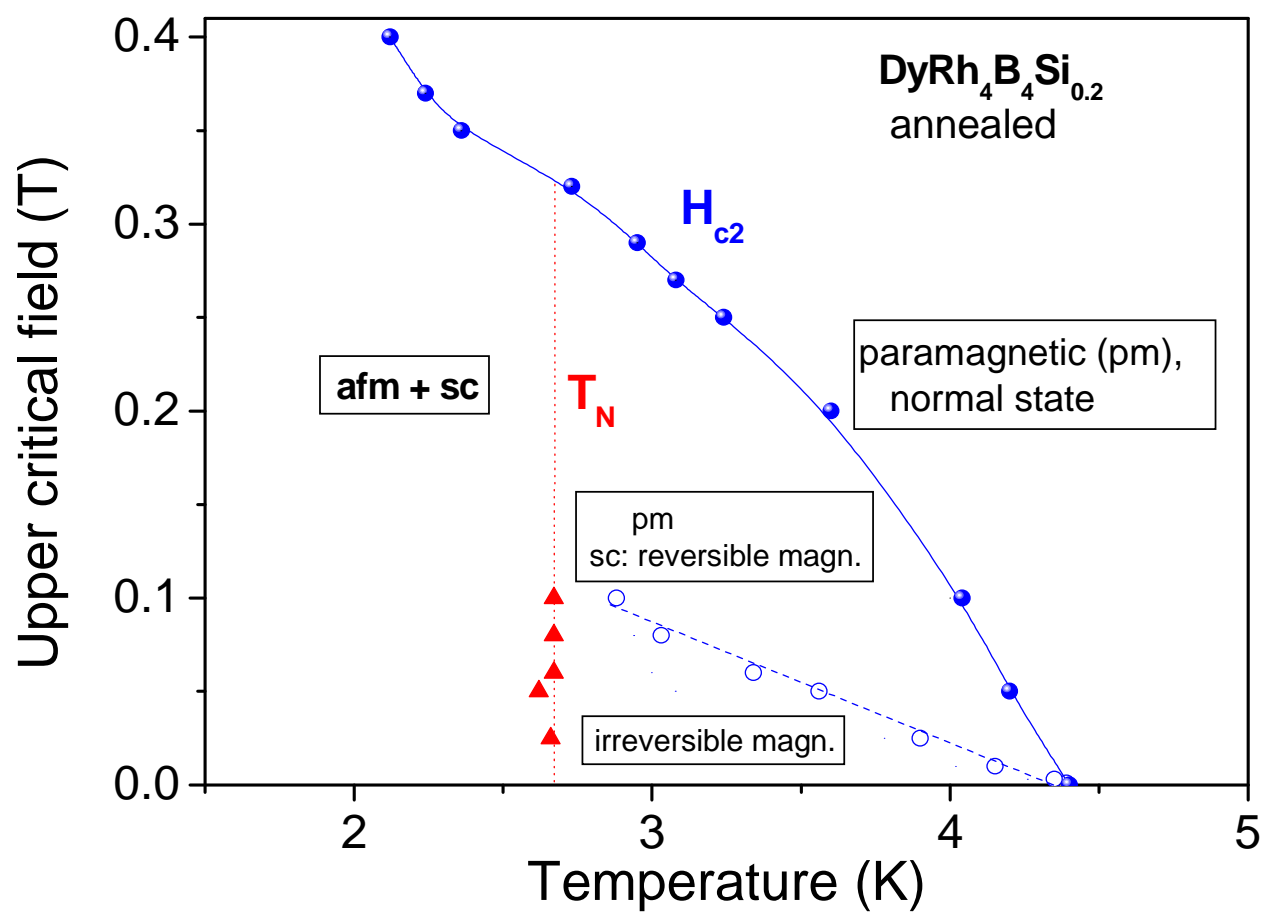


Fig. 4

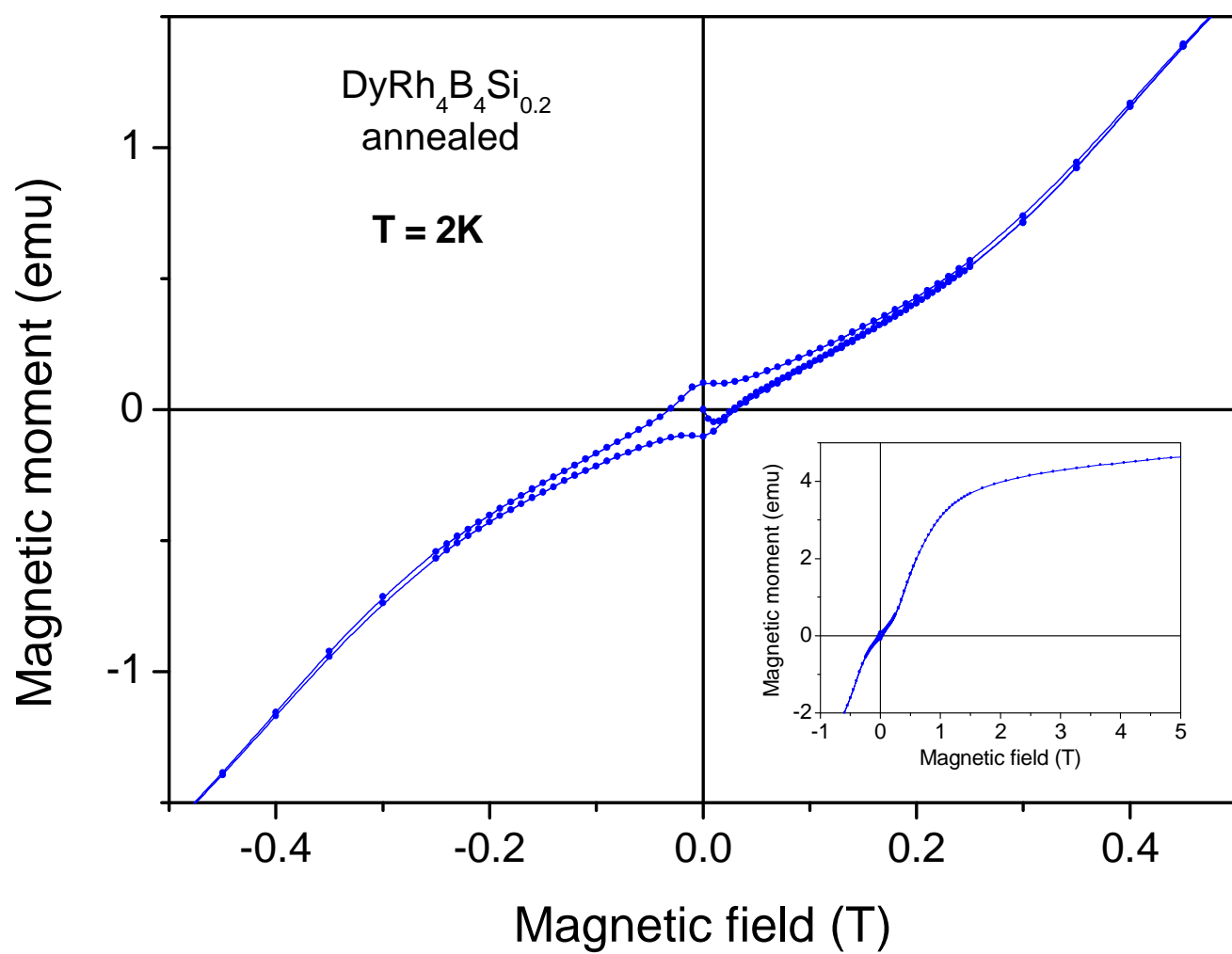


Fig. 5

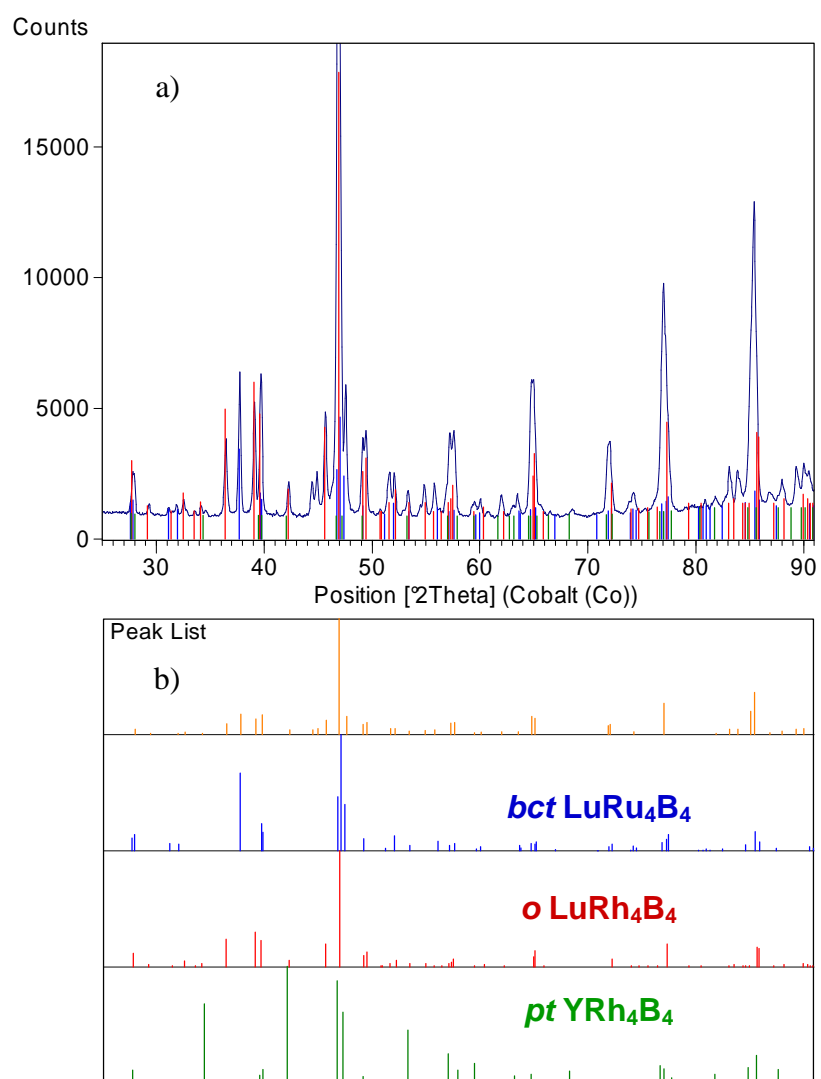


Fig. 6